博　士　論　文

Study on the role of dynamin in cytokinesis of *Dictyostelium discoideum*
（細胞性粘菌の細胞質分裂におけるダイナミンの役割に関する研究）

平成 25 年 9 月

A. Y. K. MD. Masud Rana

山口大学大学院医学系研究科

Index

Abbreviations used in this paper:

MiDAS, mitosis specific dynamin actin structure; GFP, green fluorescent protein; TIRF, total internal reflection

Summary

Dynamin has been proposed to play an important role in cytokinesis, though the nature of its contribution has remained unclear. *Dictyostelium discoideum* has five dynamin-like proteins: DymA, DymB, DlpA, DlpB and DlpC. Cells mutant for *dymA*, *dlpA*, or *dlpB* presented defects in cytokinesis that resulted in multinucleation when the cells were cultured in suspension. However, the cells could divide normally when attached to the substratum; this latter process depends on traction-mediated cytokinesis B. A dynamin GTPase inhibitor also blocked cytokinesis in suspension, suggesting an important role for dynamin in cytokinesis A, which requires a contractile ring powered by myosin II. Myosin II did not properly localize to the cleavage furrow in dynamin mutant cells, and the furrow shape was distorted. DymA and DlpA were associated with actin filaments at the furrow. Fluorescence recovery after photobleaching and a DNase I binding assay revealed that actin filaments in the contractile ring were significantly fragmented in mutant cells. Dynamin is therefore involved in the stabilization of actin filaments in the furrow, which, in turn, maintain proper myosin II organization. We conclude that the lack of these dynamins disrupts proper actomyosin organization and thereby disables cytokinesis A.

Introduction

Cytokinesis is a mechanical process that cleaves a mother cell into two daughter cells (Rappaport, 1971; Robinson & Spudich, 2000). In *Dictyostelium*, cytokinesis involves the constriction of a contractile ring at the cleavage furrow, similar to cells of higher animals. The contractile rings of these cells contain parallel filaments of actin and myosin II that are assembled under the membrane of the cleavage furrow, perpendicular to the long axis of the mitotic spindle. Active sliding between these two filament systems drives constriction (Yumura & Uyeda, 2003). Myosin II is a major motor protein that generates the constriction forces responsible for cytokinesis (Glotzer, 2001; Mabuchi & Okuno, 1977). In addition to classical cytokinesis, which depends on myosin II (cytokinesis A), *Dictyostelium* also uses a distinct method of cytokinesis (cytokinesis B), attachment-assisted mitotic cleavage, which is practiced by myosin II null cells on substrates (Nagasaki *et al.*, 2002; Neujahr *et al.*, 1997; Uyeda *et al.*, 2000; Zang *et al.*, 1997). MiDASes, large actin structures underneath nuclei, are involved in cytokinesis B in *Dictyostelium* cells (Itoh & Yumura, 2007). Cytokinesis B has also been reported in some cultured animal cells (Kanada *et al.*, 2005).

Dynamin is a large GTPase responsible for diverse cellular processes in eukaryotic cells, including the release of clathrin-dependent and -independent transport vesicles, fusion and fission of mitochondria, division of chloroplasts and peroxisomes, cell division, and resistance to viral infections (Heymann & Hinshaw, 2009; Thompson *et al.*, 2002). The soybean DRP1 homolog, phragmoplastin, was the first dynamin shown to be involved in cytokinesis (Gu & Verma, 1996). *Arabidopsis* has 16 dynamin-like proteins grouped into 6 subfamilies (DRP1-6), of which DRP2 is most closely related to mammalian dynamin 1 (Hong *et al.*, 2003). DRP1, DRP2 and DRP5 are involved in cytokinesis (Kang *et al.*, 2003; Miyagishima *et al.*, 2008).

Mammals have three classical dynamins. Dynamin 1 and dynamin 3 are expressed in a tissue-specific manner: dynamin 1 in brain and dynamin 3 in the testis, lung and heart. Dynamin 2, by contrast, is ubiquitously expressed (Ferguson & De Camilli, 2012; Tanabe & Takei, 2009). In addition, several dynamin-like proteins have been reported in mammals, including DRP1, OPA1, atlastin, mitofusin and the antiviral, interferon-inducible myxovirus resistance proteins (Ferguson & De Camilli, 2012). Among the dynamin-like proteins, DRP1 is involved in mitochondrial and peroxisomal division (Koch *et al*., 2005). In HeLa cells, dynamin 2 localizes at the spindle midzone and the subsequent intercellular bridge, suggesting an important role for this protein in the final separation of dividing cells (Chircop *et al*., 2011; Thompson *et al*., 2002). In *Caenorhabditis elegans,* dynamin (Dyn-1) localizes to the cleavage furrow and accumulates at the midbody of dividing embryos in a manner similar to that of mammalian cells. RNAi silencing of *dyn-1* in *C. elegans* embryos produced a marked defect in the late stage of cytokinesis (Thompson *et al*., 2002). The *Drosophila* dynamin homolog *shibire* localizes to sites of membrane invagination during cellularization, an alternate form of cytokinesis (Pelissier *et al*., 2003).

Classical dynamin proteins have five characteristic domains: an N-terminal GTPase domain, a middle domain, a pleckstrin homology (PH) domain, a GTPase effector domain (GED), and a C-terminal proline-rich domain (PRD). In contrast, dynamin-related proteins lack the PRD and PH domain (Praefcke & McMahon, 2004). *Dictyostelium discoideum* has five dynamin-like proteins: DymA, DymB, DlpA, DlpB and DlpC (Praefcke & McMahon, 2004; Rai *et al*., 2011; Schimmel *et al*., 2012). DymA and DymB have three domains: a GTPase domain, a middle domain and GED domain. An additional QNS (glutamine, serine and asparagine) domain is

present in DymA, and a QPS (glutamine, proline and serine) domain is present in DymB (Rai *et al*., 2011; Wienke *et al*., 1999). DlpA, DlpB and DlpC have not yet been characterized.

Phylogenetic analysis places DymA in the same branch as the yeast proteins Vps1p and Dnm1p and the mammalian proteins DRP1. The members of this group appear to support peroxisomal and mitochondrial division, vesicle trafficking and cytokinesis (Miyagishima *et al*., 2008; Rai *et al*., 2011; Wienke *et al*., 1999). DlpA, DlpB and DlpC are grouped with the plant dynamin-related proteins DRP5A and DRP5B, which are involved in cytokinesis and chloroplast division (Miyagishima *et al*., 2008). Dynamin was initially identified as a microtubule-binding protein in mammals (Shpetner & Vallee, 1989). Dynamin 2 was reported to associate with microtubules through its PRD domain (Morita *et al*., 2010) and also localizes to the mitotic spindle (Ishida *et al*., 2011).

In previous reports, *Dictyostelium* mutant cells lacking DymA showed alterations in mitochondrial, nuclear, and endosomal morphology as well as a defect in fluid-phase uptake (Wienke *et al*., 1999). However, more recently, Schimmel *et al.* reported that DymA and DymB are not essential for fission or fusion of mitochondria (Schimmel *et al*., 2012). DymB depletion affects many aspects of cell motility, cell-cell and cell-substratum adhesion, resistance to osmotic shock, and fatty acid metabolism (Rai *et al*., 2011). Previously, we showed that DlpA localized to the furrow of dividing cells (Miyagishima *et al*., 2008). However, the molecular mechanism by which these proteins contribute to cytokinesis has not been characterized to date.

In the present study, we examined knockout mutants of all of *Dictyostelium* dynamin-like genes and show that some of these proteins, actively localizing to the cleavage furrow, play important roles in cytokinesis. Several lines of experiments revealed that fragmentation of actin filaments occurred at the furrow of dividing dynamin-like protein null cells, resulting in a

significant increase in actin turnover. In *Dictyostelium* cells, dynamin-like proteins may therefore help to stabilize actin filaments in the contractile ring. We discuss how dynamin contributes to the maintenance of the contractile ring.

Materials and Methods

Cell culture

Dictyostelium discoideum AX2 wild-type cells and all mutant cells were cultured axenically in HL5 medium (1.3% bacteriological peptone, 0.75% yeast extract, 85.5 mM D-glucose, 3.5 mM Na_2HPO_4, and 3.5 mM KH_2PO_4, pH 6.4) at 22°C. Cells were cultured in suspension at 150 rpm or in plastic dishes.

Plasmid construction and transformation

Expression vectors containing EGFP-ABD120K or EGFP-myosin II heavy chain were transformed into wild-type and dynamin mutant cells by electroporation as described previously (Yumura *et al*., 1995). Positive cells were selected using 10 µg/ml G418 (Geneticin). To generate the DlpA-GFP construct, which drives the expression of DlpA fused to GFP at the C-terminus, the full-length *dlpA* gene was amplified from *Dictyostelium* genomic DNA by PCR using the following primer set, including codons for 9 glycine linkers (underlined) and BamHI sites (italics): 5'-ATC*GGATCC*AATGATATCTTGTACTAATCATCATCG-3' and 5'-ATC*GGATCC*ACCACCACCACCACCACCACCACCACCAGCAGATGGAGTTGGATTAG-3'. The PCR product was subcloned into the pA15GFP vector as a BamHI fragment, the plasmid was transformed into AX2 or *dlpA* null cells, and cells expressing DlpA-GFP were selected in the presence of G418. Knockout mutants for *dlpA, dlpB and dlpC* were generated previously (Miyagishima *et al*., 2008). Knockout mutants for *dymA* and *dymB* were newly generated by homologous recombination as previously described (Miyagishima *et al*., 2008). Myosin II null cells (HS1) were originally generated by Manstein *et al*. (Manstein *et al*., 1989).

Microscopic observation

For immunostaining with anti-myosin II (heavy chains of *Dictyostelium* myosin II) antibodies, cells were fixed as described previously (Yumura *et al.*, 1984). Briefly, cells were settled on coverslips and overlaid with an agarose sheet, followed by fixation in ethanol containing 1% formaldehyde for 5 min at -15°C. After washing with PBS (137 mM NaCl, 8 mM Na_2HPO_4, 1.47 mM KH_2PO_4, 2.7 mM KCl, 15.4 mM NaN_3, pH 7.4), the cells were immunostained with monoclonal anti-myosin II antibodies and FITC- or Alexa 488- conjugated secondary antibodies (Molecular Probes). A 5 mM solution of Dynole was prepared in dimethyl sulfoxide and stored at -20°C. For experiments, Dynole was dissolved in HL5 medium and used to observe effects on cell growth and multinucleation.

For immunostaining with anti-dynamin antibodies, cells were fixed as described previously (Miyagishima *et al*., 2008). Briefly, cells settled on coverslips were fixed in a fixative containing 2% formaldehyde, 10 mM EGTA, 5 mM $MgSO_4$, and 50 mM PIPES (pH 6.8) for 30 min at room temperature and then immersed in methanol at -20°C for 5 min. After washing with PBS for 10 min, cells were immunostained as described above.

To stain Triton X-100-extracted cells, cells were overlaid with an agarose sheet and permeabilized in Triton buffer (10 mM PIPES, 100 mM NaCl, 10 mM EGTA, 10 mM EDTA, 4 mM NaF, 0.2 mM phenylmethylsulfonyl fluoride, 2 mM dithiothreitol, 10 mM benzamidine and 1% Triton X-100, pH 7.5) for 5 min and then washed in wash buffer (5 mM PIPES,15 mM NaCl, 2 mM $MgCl_2$, 0.2 mM dithiothreitol and 0.1% NaN_3, pH 7.5). The cells were then stained with a 50 ng/ml fluorescein isothiocyanate (FITC)-conjugated phalloidin (Sigma) and a 0.1 mg/ml TRITC-DNase I (Molecular Probes) for 30 min and then washed in wash buffer. To

immunostain with anti-dynamin antibodies, the Triton X-100-extracted cells were incubated with the antibodies and fluorescent secondary antibodies.

The cells were observed by fluorescence microscopy (TE 300, Nikon) and a TIRF microscope of our composition (Yumura *et al*., 2008). Nuclei were stained with 4,6-diamidino-2-phenylindole (DAPI) as previously described (Yumura *et al*., 2005). Relative fluorescence was measured by ImageJ (http://rsb.info.nih.gov/ij/).

For live cell imaging, cells expressing DlpA-GFP or GFP-ABD 120K were overlaid with an agarose sheet, and latrunculin B (10 µM final concentration, Sigma) was applied on the agar surface while observing the dividing cells by confocal laser microscopy (LSM-510 META Zeiss) using a 60x objective lens (Plan Neofluar, NA 1.4).

Soft agarose embedding

Cell division in suspension was observed using a low melting temperature agarose embedding technique that mimics suspension conditions (Gerald *et al*., 1998; Pramanik *et al*., 2009). Cells were mixed with 0.033% (w/v) low melting temperature agarose (SIGMA) at room temperature and then rapidly placed on ice for gelation. Live cell movies were captured under phase-contrast microscopy (TE 300, Nikon).

Fluorescence recovery after photobleaching (FRAP) analysis

For FRAP experiments, wild-type and mutant cells expressing GFP-ABD120K were allowed to attach to the coverslip-bottom chamber. Live imaging and photobleaching experiments were

performed using a confocal laser scanning microscope. The half-time of fluorescence recovery was calculated as described previously (Yumura, 2001).

Polyclonal antibodies and immunoblotting

Polyclonal rabbit anti-dynamin antibodies were raised against recombinant polypeptides. Recombinant dynamin polypeptides (amino acids 203-713 for DlpA, amino acids 76-575 for DymA, amino acids 130-643 for DymB) were separately expressed in *Escherichia coli*, purified, and injected into rabbits as described previously (Miyagishima *et al*., 2008). The antiserum was absorbed by acetone powder of *E. coli* and the respective null cells before use (Miyagishima *et al*., 2008). For immunoblotting, whole cells were dissolved in 2x SDS sample buffer (0.125 M Tris pH 6.8, 4% sodium dodecyl sulfate, 20% glycerol, 0.2 M dithiothreitol, 0.02% bromophenol blue). For Triton X-100-treated samples, cells were extracted with Triton buffer on ice for 15 minutes, collected by centrifugation at 8,000 rpm, and they were then dissolved in 2x SDS sample buffer. All samples were separated on 8% SDS–polyacrylamide gels and transferred onto polyvinylidene difluoride membranes (Immobilon; Millipore) at 100 V for 2 hr. After incubating the membrane with adsorbed anti-dynamin serum followed by HRP-goat anti-rabbit IgG (Sigma), the color reaction was developed using Chemi-Lumi One L (Nacalai Tesque, JAPAN). The bands were monitored by a chemiluminescence detector (Fujifilm LAS 3000 Mini), and quantitative analysis was performed with ImageJ software.

Results

Dynamin contributes to cytokinesis

Dictyostelium has 5 dynamin-like protein genes, *dymA*, *dymB*, *dlpA*, *dlpB* and *dlpC*. For simplicity, we will refer to dynamin-like proteins as dynamins. To investigate the role of *Dictyostelium* dynamins in cell division, we examined the growth of knockout mutant cells for each genes. The number of *dlpA, dlpB* and *dymA* null cells increased more slowly than that of wild-type cells (AX2) in suspension culture. *dymA* null cells showed the most severe defects in suspension among the five mutant cell lines (Fig. 1A). However, when cultured on plastic dishes, the growth of mutant cells was normal or only slightly slower than that of wild-type cells (Fig.1B).

When wild-type cells were cultured in a nutrient medium containing Dynole, a dynamin GTPase inhibitor, they also showed remarkable growth defects in suspension (Fig. 1A). The doubling time of wild-type cells in suspension was 24.8 hrs in the presence of 4 μM Dynole but only 9.8 hrs for untreated cells. At concentrations higher than 6 μM, Dynole had a cytotoxic effect.

Figure 1C shows the nuclei of mutant cells stained with DAPI. When cultured in suspension, the size of mutant cells, especially *dymA*, *dlpA* and *dlpB* null cells, was much larger than that of wild-type cells, and they contained multiple nuclei. In *dymA*, *dlpA* and *dlpB* null cells, multinucleation was noted particularly frequently in suspension (Fig. 1D). When wild-type cells were cultured in suspension in the presence of Dynole, they also increased in size and presented multiple nuclei. Fig. 1E shows a dose-response curve for Dynole-induced multinucleation. Thus, the deletion or inhibition of dynamin activity results in defective cytokinesis in suspension.

To determine why the cells failed to divide in suspension, dynamin null cells were embedded

in low melting temperature agarose which mimics suspension conditions. Figure 1F shows typical failures of cell division of *dymA* null cells embedded in agarose. A bulging structure with double furrows was observed in unsuccessfully dividing *dymA* null cells (arrows in right panel of Fig. 1F, see also Fig. 4). In some cases (~10%), dividing *dymA* null cells produced two halves with an interconnected cytoplasmic thread, which later fused, causing the cells to become binucleate (left panels of Fig. 1F). *dlpA* and *dlpB* null cells also failed to achieve cytokinesis in a similar fashion as *dymA* null cells.

Dynamin localizes to the furrow of dividing cells

The intracellular distribution of DymA and DlpA was previously examined in *Dictyostelium* cells. Wienke *et al.* showed that DymA colocalized with the Golgi complex in interphase cells (Wienke *et al*., 1999). We previously showed by immunostaining that DlpA localizes to the cleavage furrow of dividing cells (Miyagishima *et al*., 2008). In the present study, we produced new specific antibodies against DymA and DymB. As we previously showed, immunostaining with anti-DlpA antibodies clearly showed localization at the cleavage furrow (Fig. 2A and B). DymA also localized to the furrow region (Fig. 2C-F). However, DymB was diffusely distributed throughout the cytoplasm (Fig. 2G and H).

To observe the dynamics of DlpA in live cells, we made a GFP-DlpA expression construct in which GFP was fused to the N-terminus of *dlpA*. Upon expression in living cells, the fused protein tended to aggregate and showed no localization at the cleavage furrow. We then fused GFP to the C-terminus of *dlpA*. This DlpA-GFP began to accumulate at the equator at late anaphase and localized along the contractile ring during cytokinesis, similar to the pattern observed by immunostaining (Fig. 3A and B). Expression of DlpA-GFP in *dlpA* null cells

rescued multinucleation (data not shown). These results indicate that DlpA and DymA localize at the furrow and contribute to cytokinesis.

Dynamin knockout induces aberrant localization of myosin II at the furrow

Our observation that knockout of dynamin genes or application of the dynamin inhibitor reduced cell growth only in suspension culture was reminiscent of myosin II null cells. Myosin II null cells cannot grow in suspension and become multinucleated due to defects in the constriction of the contractile ring, although they can still divide on surfaces using traction force (cytokinesis B) (Nagasaki *et al*., 2002; Zang *et al*., 1997). The defects of dynamin knockout cells may therefore be related to myosin II activity. We examined myosin II localization in dividing mutant cells by immunofluorescence. As we previously showed (Yumura *et al*., 1984), myosin II localized to the cleavage furrow in dividing wild-type cells (Fig. 4A and B).

In *dlpA* null cells, 26% (7/27) of examined cells were indistinguishable from wild-type cells in terms of cell morphology and localization of myosin II at the furrow. However, 41% (11/27) of the mutant cells showed normal morphology but punctate or patchy myosin localization (Fig. 4C and D). Finally, 33% (9/27) of the mutant cells had a swelling or bulge-like structure at the furrow region and showed punctate or patchy myosin localization (Fig. 4E and F).

Regarding *dymA* null cells, 18% (6/34) of examined cells were indistinguishable from wild-type cells in terms of morphology and localization of myosin II at the furrow. However, 15% (5/34) of the mutant cells showed normal morphology but punctate or patchy myosin localization (Fig. 4G and H), and 67% (23/34) of the mutant cells had a swelling or bulge-like structure at the furrow region and punctate or patchy myosin localization (Fig. 4I and J).

When wild-type cells were treated with Dynole, most (25/27) developed a swelling or bulge-like structure at the furrow region and presented punctate or patchy myosin localization (Fig. 4K and L).

The fluorescence level of myosin II at the furrow was quantitatively examined in these cells (Fig. 4M). The relative fluorescence intensity at the furrow was indistinguishable between wild-type and *dlpA* null cells. However, *dymA* null cells showed slightly but significantly lower accumulation of myosin II at the furrow, and Dynole-treated cells exhibited significantly lower myosin II levels than wild-type cells.

These observations suggest that defects in dynamin activity result in aberrant localization of myosin II at the furrow, which may cause failure of cytokinesis.

Localization of dynamin is independent of myosin II

As described above, dynamin contributes to the proper localization of myosin II at the furrow region. To determine whether myosin II also regulates dynamin localization, we evaluated dynamin localization in myosin II null cells. Dividing myosin II null cells (HS1) were immunostained with anti-DymA and DlpA antibodies. Both DymA and DlpA were properly localized at the cleavage furrow (Fig. 2I-P). Therefore, DymA and DlpA localization at the furrow is independent of the presence of myosin II.

Actin filaments are disorganized in dividing dynamin mutant cells

Actin filaments also accumulate at the furrow region in dividing cells. To evaluate actin filament organization in the absence of dynamin, mutant cells were fixed and stained with TRITC-phalloidin and then observed under total internal reflection fluorescence (TIRF)

microscopy. Actin filaments were well organized at the furrow region in dividing wild-type cells, but in *dymA* and *dlpA* null cells, actin filaments were shortened or fragmented and disorganized at the furrow (Fig. 5A).

We previously reported mitosis-specific dynamic actin structures (MiDASes) in myosin II null cells (Itoh & Yumura, 2007), which appear beneath the nuclei during mitosis as sites of adhesion to the substratum. MiDASes provide a strong scaffold and mechanical force against the substratum for cytokinesis B. Interestingly, MiDASes were found in 70% (21/30) of *dlpA* null cells growing on a surface (arrows in Fig. 5A). MiDASes were also found in *dymA* (10-20%) and *dlpB* (10-20%) null cells. That MiDASes were found in both myosin II null and dynamin null cells suggests that dynamin is required for the appropriate activity or organization of myosin II. Dynamin null cells may therefore divide on surfaces predominantly via cytokinesis B rather than cytokinesis A.

Dynamin is associated with actin filaments at the furrow

The observed colocalization of actin and dynamin at the cleavage furrow indicates that these proteins may associate with each other. To further examine this possibility, cells were extracted with a buffer containing Triton X-100 to remove soluble proteins. After extraction, DlpA was still present and remained colocalized with the residual actin cytoskeleton (Fig. 5B). However, relatively weak localization was observed for DymA after extraction. We also performed immunoblotting on Triton X-100-extracted cells. Approximately 87% of DlpA and 41% of DymA remained associated with the cytoskeleton after extraction with Triton X-100, respectively (Fig. 5C).

We next measured the effect of latrunculin B, an actin-depolymerizing agent, on dividing cells expressing DlpA-GFP or GFP-ABD 120K. GFP-ABD 120K (GFP-actin-binding domain of *Dictyostelium* ABP120K) was used as a marker to visualize actin filaments (Pang *et al*., 1998). During cell division, both GFP proteins localized to the furrow. When the cells were exposed to latrunculin B, DlpA-GFP and GFP-ABD 120K delocalized from the furrow in a similar manner, and the furrows themselves eventually loosened (Fig. 6A and B).

These observations indicate that DlpA is associated with actin filaments at the cleavage furrow.

Dynamin stabilizes actin filaments at the furrow

To further investigate the apparent fragmentation of actin filaments at the furrow of dividing mutant cells, we performed TRITC-DNase I staining. DNase I binds to the pointed ends of actin filaments as well as subdomains II and IV of monomeric actin (Podolski & Steck, 1988; Kabsch *et al.*, 1990). If actin filaments are fragmented at the furrow, we predicted that there would be more free ends of actin filaments available for binding TRITC-DNase I. After extracting the cells with Triton X-100 in an actin-stabilizing solution, the residual cytoskeleton was simultaneously stained with TRITC-DNase I and FITC-phalloidin. Monomeric actin was substantially extracted under these conditions. Interestingly, furrow regions were mainly stained with TRITC-DNase I, whereas FITC-phalloidin stained both polar pseudopods and the furrow (Fig. 7A). A quantitative analysis of the fluorescence of bound FITC-phalloidin revealed no significant differences in the amount of actin filaments at the furrow region between wild-type and mutant cells. However, the relative fluorescence intensity of bound TRITC-DNase I at the furrow was much higher in both *dymA* and *dlpA* mutant cells than in wild-type cells (Fig. 7B).

These results suggest that the number of shorter actin filaments is increased at the furrow region of mutant cells.

To further confirm the fragmentation of actin filaments in mutant cells, fluorescence recovery after photobleaching (FRAP) experiments were performed at the furrow of *dlpA* null cells expressing GFP-ABD120K. If increased numbers of shorter actin filaments with free terminal ends are present at the furrow of mutant cells, filament turnover should occur more rapidly in mutant relative to wild-type cells. Previously we used GFP-ABD120K for the estimation of the turnover of actin filaments and proved that the turnover of GFP-ABD120K reflects the turnover of actin filaments (Yumura *et al.*, 2013). In the case of dividing *dlpA* null cells, the half-time of fluorescence recovery was 0.88±0.17 seconds (n=15), whereas it was 1.1±0.23 seconds (n=18) in wild-type cells (Fig. 7 C-F). Actin turnover was therefore significantly faster ($p<0.001$) in *dlpA* null compared with wild-type cells.

Taken together, actin filaments were significantly fragmented and turned over more rapidly in dynamin mutants relative to wild-type cells. Dynamin thus functions to stabilize actin filaments in the contractile ring by suppressing the extent of filament fragmentation and maintaining the proper organization of myosin II in the furrow.

Discussion

In the present study, we found that most dynamin null cells showed some defects of cytokinesis in suspension, as did wild-type cells treated with a dynamin inhibitor in suspension. DlpA and DymA clearly localized to the furrow region. These results all indicate that these dynamins are crucial for cytokinesis A in *Dictyostelium* cells. *dlpB* null cells also showed defects of cytokinesis and its localization remained to be studied in future. DlpC and DymB did not show defects of cytokinesis. They may play other roles such as maintenance of membranous organelles (Rai *et al.*, 2011).

Individual disruptions of *dymA*, *dlpA*, and *dlpB* genes all resulted in severe defects in cytokinesis in suspension. This is somewhat puzzling and two different explanations seem possible; one is that DymA, DlpA and DlpB contribute to efficient cytokinesis through separate mechanisms that are all needed for efficient cytokinesis, and the other is that all three dynamins are involved in one common mechanism and loss of any one of them inhibits the mechanism to a similar extent. The former explanation seems inconsistent with the observation that the loss of any one of them resulted in multinucleation to the extent similar to that achieved by the dynamin GTPase inhibitor Dynole. The latter explanation is compatible with the fact that dynamins function as polymers. Whether different dynamins can form a copolymer has to be examined in future.

Previous studies in a variety of organisms have shown that dynamin plays an important role in cytokinesis (Konopka *et al*., 2006). *Drosophila* carrying mutations in the dynamin homolog, *shibire*, cannot complete cytokinesis (Pelissier *et al*., 2003). Temperature-sensitive (ts) mutants for the *C. elegans* dynamin homolog, *dyn-1-ts*, present a failure of late cytokinesis (Clark *et al*., 1997). In *Arabidopsis*, *drp1a/ drp1e* double knockout embryos display defects in cytokinesis

(Kang *et al*., 2003). These studies primarily focused on dynamin's role in membrane trafficking. However, dynamin is not only localized to the membrane interface but is also present in actin-rich structures, such as lamellipodia, membrane ruffles, podosomes and invadopodia (Orth & McNiven, 2003).

In the present work, DlpA and DymA colocalized with actin filaments at the furrow, and a major fraction of dynamin remained associated with the Triton X-100-insoluble cytoskeleton. In addition, live imaging showed that the dynamins delocalized from the furrow region upon treatment of cells with latrunculin B, in accordance with the delocalization of actin filaments. These results indicate that dynamin is directly or indirectly associated with actin filaments at the furrow. Recent *in vitro* and *in vivo* studies have shown that dynamin can indirectly bind to actin filaments and modulate their assembly. Dynamin 2 interacts with actin filaments indirectly by binding to several actin-binding proteins, such as cortactin, the Arp2/3 complex (Krueger *et al*., 2003; Mooren *et al*., 2009), intersectin-1, Tuba (Hussain *et al*., 1999; Salazar *et al*., 2003), BAR, and F-Bar proteins (Rao *et al*., 2010). Dynamin 1 also binds to profilin (Witke *et al*., 1998), which is essential for actin assembly. The interaction between dynamin and these actin-modulating proteins is mediated by the PRD domain of dynamin (Anggono *et al*., 2006; Shpetner *et al*., 1996). Recently, Gu *et al*. (2010) identified a highly conserved site in the middle domain (399-444) of dynamin 2 that directly binds to actin filaments and aligns them into bundles. The authors reported that short actin filaments stimulate dynamin to self-assemble into oligomerized ring structures, which, in turn, efficiently release the actin-capping protein gelsolin from barbed ends *in vitro*, allowing elongation of actin filaments. Although these observations indicate the possibility that dynamin may function in the organization of actin structures independently of its

role in membrane remodeling, membrane remodeling also seems to be linked to the cytoskeleton, as described below.

Endocytosis has been implicated in and linked to cytokinesis. The continuance of endocytosis is crucial for cytokinesis of zebrafish blastomeres because endocytosis inhibitors block the separation of daughter cells (Feng *et al*., 2002). Clathrin was the first trafficking protein shown to be essential for cytokinesis in *Dictyostelium* (Gerald *et al*., 2001). In suspension culture, clathrin null cells developed irregular double furrows with a bulge at the equator and eventually failed to divide, similar to the phenomenon observed in dynamin null cells in the present study. Clathrin null cells also showed defects in myosin organization (Gerald *et al*., 2001). *Dictyostelium* LvsA, a novel protein which is related to the membrane trafficking, is required for cytokinesis (Kwak *et al*., 1999). These observations collectively suggest that LvsA, clathrin and dynamin may participate in a common pathway required for cytokinesis. Mutations in clathrin and dynamin also lead to cytokinesis failure in other organisms, such as *C. elegans*, *Drosophila*, and mammalian cells (Konopka *et al*., 2006).

In the present study, TRITC-DNase I primarily stained the furrow region but not the polar pseudopods of dividing cells, although actin filaments were present in both regions, as revealed by staining with FITC-phalloidin. DNase I preferentially binds to the pointed ends of actin filaments (Podolski & Steck, 1988). The pointed ends of actin filaments in pseudopods are commonly bound to Arp2/3 complexes and are thus not free, which may explain why DNase I did not stain actin filaments in the pseudopods. Conversely, the pointed ends of actin filaments at the furrow must be free.

Actin turnover in the contractile ring of *Dictyostelium* cells was examined for the first time in the present study. The half-time of recovery was approximately 1 sec, which is very fast

compared with that at contractile rings in yeast (>30 sec) (Pelham & Chang, 2002) and cultured animal cells (26-58 sec) (Kondo *et al*., 2011; Murthy & Wadsworth, 2005). In *Dictyostelium* cells, the turnover of myosin II in the contractile ring is much slower (half-time of approximately 7 sec) than that of actin and is regulated by the phosphorylation of myosin heavy chains, independently of actin turnover (Yumura *et al*., 2008; Yumura, 2001). This rapid turnover of actin and myosin II must be required for the maintenance of the contractile ring. Actin filaments at the furrow are most likely present in a relatively short form with free pointed ends, which results in rapid turnover. Actin-binding proteins that sever actin filaments, such as severin and ADF-cofillin (Chen & Pollard, 2011), are possible candidates responsible for the shorter actin filaments at the furrow. The fact that DymA and DlpA null cells showed faster turnover of actin than wild-type cells indicates that these dynamins are likely responsible for antagonizing filament severing activities, thereby helping to stabilize actin filaments in the contractile ring. Alternatively, dynamin may promote actin polymerization as described above (Gu *et al*., 2010) and maintain a constant length of actin filaments in the contractile ring. At present, it is unclear whether DlpA and DymA bind to actin filaments directly. Homology search indicates that DymA has 51% homology to the conserved actin-binding domain in the middle domain of dynamin 2 (Gu *et al*., 2010), but DlpA and DlpB have no such region. The domains of these proteins responsible for binding to actin filaments and localization at the furrow remain to be elucidated.

Myosin II can also fragment actin filaments (Haviv *et al*., 2008), which may contribute to the observed rapid turnover of actin in the contractile ring (Yumura *et al*., 2008). Our preliminary experiments suggested that actin filament turnover was decreased at the furrow of myosin II null cells. The significantly fragmented actin filaments present in dynamin null cells may lead to

irrelevant and local contractions of actomyosin, which could cause aberrant and patchy localization of myosin II at the furrow (Fig. 2), finally resulting in the failure of cytokinesis A (Fig. 8).

In the present study, dynamin null cells divided on surfaces at almost a normal rate. *Dictyostelium* cells possess the alternative division mechanism of cytokinesis B, which has also been reported in animal cells (Kanada *et al*., 2005; Uyeda *et al*., 2000). Deficiency of cytokinesis A may activate cytokinesis B under these conditions because MiDASes were frequently observed in myosin II null and dynamin null cells. However, the molecular mechanism underlying the switch from cytokinesis A to cytokinesis B remains unclear, as does the mechanism by which cells sense whether they are capable of undergoing cytokinesis A.

In summary, the *Dictyostelium* dynamin-like proteins DymA and DlpA localize to the cleavage furrow and associate with actin filaments, helping to maintain filaments of the appropriate length. These dynamins also contribute to the stabilization of actin filaments in the furrow, which, in turn, maintains proper myosin II organization. Deficiency of these dynamins disturbs actomyosin organization and disables cytokinesis A, resulting in the induction of MiDASes and promotion of cytokinesis B.

References

Anggono, V., Smillie, K. J., Graham, M. E., Valova, V. A., Cousin, M. A. and Robinson, P. J. (2006) Syndapin I is the phosphorylation-regulated dynamin I partner in synaptic vesicle endocytosis. *Nat Neurosci.* **9,** 752-760.

Chen, Q. and Pollard, T. D. (2011) Actin filament severing by cofilin is more important for assembly than constriction of the cytokinetic contractile ring. *J Cell Biol.* **195,** 485-498.

Chircop, M., Sarcevic, B., Larsen, M. R. *et al*. (2011) Phosphorylation of dynamin II at serine-764 is associated with cytokinesis. *Biochim Biophys Acta.* **1813,** 1689-1699.

Clark, S. G., Shurland, D. L., Meyerowitz, E. M., Bargmann, C. I. and van der Bliek, A. M. (1997) A dynamin GTPase mutation causes a rapid and reversible temperature-inducible locomotion defect in C. elegans. *Proc Natl Acad Sci U S A.* **94,** 10438-10443.

Feng, B., Schwarz, H. and Jesuthasan, S. (2002) Furrow-specific endocytosis during cytokinesis of zebrafish blastomeres. *Exp Cell Res.* **279,** 14-20.

Ferguson, S. M. and De Camilli, P. (2012) Dynamin, a membrane-remodelling GTPase. *Nat Rev Mol Cell Biol.* **13,** 75-88.

Gerald, N., Dai, J., Ting-Beall, H. P. and De Lozanne, A. (1998) A role for *Dictyostelium* racE in cortical tension and cleavage furrow progression. *J Cell Biol.* **141,** 483-492.

Gerald, N. J., Damer, C. K., O'Halloran, T. J. and De Lozanne, A. (2001) Cytokinesis failure in clathrin-minus cells is caused by cleavage furrow instability. *Cell Motil Cytoskeleton.* **48,** 213-223.

Glotzer, M. (2001) Animal cell cytokinesis. *Annu Rev Cell Dev Biol.* **17,** 351-386.

Gu, C., Yaddanapudi, S., Weins, A., Osborn, T., Reiser, J., Pollak, M., Hartwig, J. and Sever, S. (2010) Direct dynamin-actin interactions regulate the actin cytoskeleton. *EMBO J.* **29,** 3593-3606.

Gu, X. and Verma, D. P. (1996) Phragmoplastin, a dynamin-like protein associated with cell plate formation in plants. *EMBO J.* **15,** 695-704.

Haviv, L., Gillo, D., Backouche, F. and Bernheim-Groswasser, A. (2008) A cytoskeletal demolition worker: myosin II acts as an actin depolymerization agent. *J Mol Biol.* **375,** 325-330.

Heymann, J. A. and Hinshaw, J. E. (2009) Dynamins at a glance. *J Cell Sci.* **122,** 3427-3431.

Hong, Z., Bednarek, S. Y., Blumwald, E. *et al*. (2003) A unified nomenclature for *Arabidopsis* dynamin-related large GTPases based on homology and possible functions. *Plant Mol Biol.* **53(3),** 261-265.

Hussain, N. K., Yamabhai, M., Ramjaun, A. R., Guy, A. M., Baranes, D., O'Bryan, J. P., Der, C. J., Kay, B. K. and McPherson, P. S. (1999) Splice variants of intersectin are components of the endocytic machinery in neurons and nonneuronal cells. *J Biol Chem.* **274,** 15671-15677.

Ishida, N., Nakamura, Y., Tanabe, K., Li, S. A. and Takei, K. (2011) Dynamin 2 associates with microtubules at mitosis and regulates cell cycle progression. *Cell Struct Funct.* **36,** 145-154.

Itoh, G. and Yumura, S. (2007) A novel mitosis-specific dynamic actin structure in *Dictyostelium* cells. *J Cell Sci.* **120,** 4302-4309.

Kabsch, W., Mannherz, H. G., Suck, D., Pai, E. F. and Holmes, K. C. (1990) Atomic structure of the actin:DNase I complex. *Nature.* **347,** 37-44.

Kanada, M., Nagasaki, A. and Uyeda, T. Q. (2005) Adhesion-dependent and contractile ring-independent equatorial furrowing during cytokinesis in mammalian cells. *Mol Biol Cell.* **16,** 3865-3872.

Kang, B. H., Busse, J. S. and Bednarek, S. Y. (2003) Members of the *Arabidopsis* dynamin-like gene family, ADL1, are essential for plant cytokinesis and polarized cell growth. *Plant Cell.* **15,** 899-913.

Koch, A., Yoon, Y., Bonekamp, N. A., McNiven, M. A. and Schrader, M. (2005) A role for Fis1 in both mitochondrial and peroxisomal fission in mammalian cells. *Mol Biol Cell.* **16,** 5077-5086.

Kondo, T., Hamao, K., Kamijo, K., Kimura, H., Morita, M., Takahashi, M. and Hosoya, H. (2011) Enhancement of myosin II/actin turnover at the contractile ring induces slower furrowing in dividing HeLa cells. *Biochem J.* **435,** 569-576.

Konopka, C. A., Schleede, J. B., Skop, A. R. and Bednarek, S. Y. (2006) Dynamin and cytokinesis. *Traffic.* **7,** 239-247.

Krueger, E. W., Orth, J. D., Cao, H. and McNiven, M. A. (2003) A dynamin-cortactin-Arp2/3 complex mediates actin reorganization in growth factor-stimulated cells. *Mol Biol Cell.* **14,** 1085-1096.

Kwak, E., Gerald, N., Larochelle, D. A., Vithalani, K. K., Niswonger, M. L., Maready, M. and De Lozanne, A. (1999) LvsA, a protein related to the mouse beige protein, is required for cytokinesis in *Dictyostelium*. *Mol Biol Cell.* **10,** 4429-4439.

Mabuchi, I. and Okuno, M. (1977) The effect of myosin antibody on the division of starfish blastomeres. *J Cell Biol.* **74,** 251-263.

Manstein, D. J., Titus, M. A., De Lozanne, A. and Spudich, J. A. (1989) Gene replacement in *Dictyostelium*: generation of myosin null mutants. *EMBO J.* **8,** 923-932.

Miyagishima, S. Y., Kuwayama, H., Urushihara, H. and Nakanishi, H. (2008) Evolutionary linkage between eukaryotic cytokinesis and chloroplast division by dynamin proteins. *Proc Natl Acad Sci U S A.* **105,** 15202-15207.

Mooren, O. L., Kotova, T. I., Moore, A. J. and Schafer, D. A. (2009) Dynamin2 GTPase and cortactin remodel actin filaments. *J Biol Chem.* **284,** 23995-24005.

Morita, M., Hamao, K., Izumi, S., Okumura, E., Tanaka, K., Kishimoto, T. and Hosoya, H. (2010) Proline-rich domain in dynamin-2 has a low microtubule-binding activity: how is this activity controlled during mitosis in HeLa cells? *J Biochem.* **148,** 533-538.

Murthy, K. and Wadsworth, P. (2005) Myosin-II-dependent localization and dynamics of F-actin during cytokinesis. *Curr Biol.* **15,** 724-731.

Nagasaki, A., de Hostos, E. L. and Uyeda, T. Q. (2002) Genetic and morphological evidence for two parallel pathways of cell-cycle-coupled cytokinesis in *Dictyostelium*. *J Cell Sci.* **115,** 2241-2251.

Neujahr, R., Heizer, C. and Gerisch, G. (1997) Myosin II-independent processes in mitotic cells of *Dictyostelium discoideum*: redistribution of the nuclei, re-arrangement of the actin system and formation of the cleavage furrow. *J Cell Sci.* **110,** 123-137.

Orth, J. D. and McNiven, M. A. (2003) Dynamin at the actin-membrane interface. *Curr Opin Cell Biol.* **15,** 31-39.

Pang, K. M., Lee, E. and Knecht, D. A. (1998) Use of a fusion protein between GFP and an actin-binding domain to visualize transient filamentous-actin structures. *Curr Biol.* **8,** 405-408.

Pelham, R. J. and Chang, F. (2002) Actin dynamics in the contractile ring during cytokinesis in fission yeast. *Nature.* **419,** 82-86.

Pelissier, A., Chauvin, J. P. and Lecuit, T. (2003) Trafficking through Rab11 endosomes is required for cellularization during *Drosophila* embryogenesis. *Curr Biol.* **13,** 1848-1857.

Podolski, J. L. and Steck, T. L. (1988) Association of deoxyribonuclease I with the pointed ends of actin filaments in human red blood cell membrane skeletons. *J Biol Chem.* **263,** 638-645.

Praefcke, G. J. and McMahon, H. T. (2004) The dynamin superfamily: universal membrane tubulation and fission molecules? *Nat Rev Mol Cell Biol.* **5,** 133-147.

Pramanik, M. K., Iijima, M., Iwadate, Y. and Yumura, S. (2009) PTEN is a mechanosensing signal transducer for myosin II localization in *Dictyostelium* cells. *Genes Cells.* **14,** 821-834.

Rai, A., Nothe, H., Tzvetkov, N., Korenbaum, E. and Manstein, D. J. (2011) *Dictyostelium* dynamin B modulates cytoskeletal structures and membranous organelles. *Cell Mol Life Sci.* **68,** 2751-2767.

Rao, Y., Ma, Q., Vahedi-Faridi, A., Sundborger, A., Pechstein, A., Puchkov, D., Luo, L., Shupliakov, O., Saenger, W. and Haucke, V. (2010) Molecular basis for SH3 domain regulation of F-BAR-mediated membrane deformation. *Proc Natl Acad Sci U S A.* **107,** 8213-8218.

Rappaport, R. (1971) Cytokinesis in animal cells. *Int Rev Cytol.* **31,** 169-213.

Robinson, D. N. and Spudich, J. A. (2000) Towards a molecular understanding of cytokinesis. *Trends Cell Biol.* **10,** 228-237.

Salazar, M. A., Kwiatkowski, A. V., Pellegrini, L., Cestra, G., Butler, M. H., Rossman, K. L., Serna, D. M., Sondek, J., Gertler, F. B. and De Camilli, P. (2003) Tuba, a novel protein containing bin/amphiphysin/Rvs and Dbl homology domains, links dynamin to regulation of the actin cytoskeleton. *J Biol Chem.* **278,** 49031-49043.

Schimmel, B. G., Berbusse, G. W. and Naylor, K. (2012) Mitochondrial fission and fusion in *Dictyostelium discoideum*: a search for proteins involved in membrane dynamics. *BMC Res Notes.* **5,** 505.

Shpetner, H. S., Herskovits, J. S. and Vallee, R. B. (1996) A binding site for SH3 domains targets dynamin to coated pits. *J Biol Chem.* **271,** 13-16.

Shpetner, H. S. and Vallee, R. B. (1989) Identification of dynamin, a novel mechanochemical enzyme that mediates interactions between microtubules. *Cell.* **59,** 421-432.

Tanabe, K. and Takei, K. (2009) Dynamic instability of microtubules requires dynamin 2 and is impaired in a Charcot-Marie-Tooth mutant. *J Cell Biol.* **185,** 939-948.

Thompson, H. M., Skop, A. R., Euteneuer, U., Meyer, B. J. and McNiven, M. A. (2002) The large GTPase dynamin associates with the spindle midzone and is required for cytokinesis. *Curr Biol.* **12,** 2111-2117.

Uyeda, T. Q., Kitayama, C. and Yumura, S. (2000) Myosin II-independent cytokinesis in *Dictyostelium*: its mechanism and implications. *Cell Struct Funct.* **25,** 1-10.

Wienke, D. C., Knetsch, M. L., Neuhaus, E. M., Reedy, M. C. and Manstein, D. J. (1999) Disruption of a dynamin homologue affects endocytosis, organelle morphology, and cytokinesis in *Dictyostelium discoideum*. *Mol Biol Cell.* **10,** 225-243.

Witke, W., Podtelejnikov, A. V., Di Nardo, A., Sutherland, J. D., Gurniak, C. B., Dotti, C. and Mann, M. (1998) In mouse brain profilin I and profilin II associate with regulators of the endocytic pathway and actin assembly. *EMBO J.* **17,** 967-976.

Yumura, S. (2001) Myosin II dynamics and cortical flow during contractile ring formation in *Dictyostelium* cells. *J Cell Biol.* **154,** 137-146.

Yumura, S., Itoh, G., Kikuta, Y., Kikuchi, T., Kitanishi-Yumura, T. and Tsujioka, M. (2013) Cell-scale dynamic recycling and cortical flow of the actin-myosin cytoskeleton for rapid cell migration. *Biol Open.* **2,** 200-209.

Yumura, S., Matsuzaki, R. and Kitanishi-Yumura, T. (1995) Introduction of macromolecules into living *Dictyostelium* cells by electroporation. *Cell Struct Funct.* **20,** 185-190.

Yumura, S., Mori, H. and Fukui, Y. (1984) Localization of actin and myosin for the study of ameboid movement in *Dictyostelium* using improved immunofluorescence. *J Cell Biol.* **99,** 894-899.

Yumura, S., Ueda, M., Sako, Y., Kitanishi-Yumura, T. and Yanagida, T. (2008) Multiple mechanisms for accumulation of myosin II filaments at the equator during cytokinesis. *Traffic.* **9,** 2089-2099.

Yumura, S. and Uyeda, T. Q. (2003) Myosins and cell dynamics in cellular slime molds. *Int Rev Cytol.* **224,** 173-225.

Yumura, S., Yoshida, M., Betapudi, V., Licate, L. S., Iwadate, Y., Nagasaki, A., Uyeda, T. Q. and Egelhoff, T. T. (2005) Multiple myosin II heavy chain kinases: roles in filament assembly control and proper cytokinesis in *Dictyostelium*. *Mol Biol Cell.* **16,** 4256-4266.

Zang, J. H., Cavet, G., Sabry, J. H., Wagner, P., Moores, S. L. and Spudich, J. A. (1997) On the role of myosin-II in cytokinesis: division of *Dictyostelium* cells under adhesive and nonadhesive conditions. *Mol Biol Cell.* **8,** 2617-2629.

Acknowledgments

I would like to express my gratitude to my supervisor Professor Dr. Shigehiko Yumura for his guidance throughout my research and writing this thesis paper. I am grateful to Dr. Shinya Miyagishima and Dr. Masatsune Tsujioka for their help in my research. I would also like to thank Dr. T. Q. P. Uyeda and Dr. T. Kitanishi-Yumura for valuable discussions. I am also thankful to Newcastle Innovation/CMRI for supplying Dynole. I wish to thank to Mr. Koushirou Fujimoto and other students of our laboratory throughout my research period.

Fig. 1. Dynamin null cells failed to complete cytokinesis in suspension culture. (A) Growth curves of five dynamin null cell lines growing in suspension. (B) Growth curves of five dynamin null cell lines on a surface. Dynole, a dynamin GTPase inhibitor, was applied at a concentration of 4 μM. (C) DAPI staining of wild-type cells and five dynamin null mutant lines after 3 days of culture on a surface or in suspension. The bottom images show DAPI staining of wild-type cells grown in the presence of Dynole for 3 days. (D) Comparison of the percentage of multinucleation among dynamin null cells and AX2 wild-type cells on surface and suspension conditions. The number of nuclei of more than 200 cells was examined for each case. Multinucleation in dynamin null cells was observed more frequently in suspension than on a surface. (E) A dose-response curve for Dynole-induced multinucleation. (F) Two examples of sequential images show that *dymA* null cells failed to divide in low melting temperature agarose, which mimics suspension conditions. White arrows indicate a double furrow (right panel). See also Fig. 4. Bars, 10 μm.

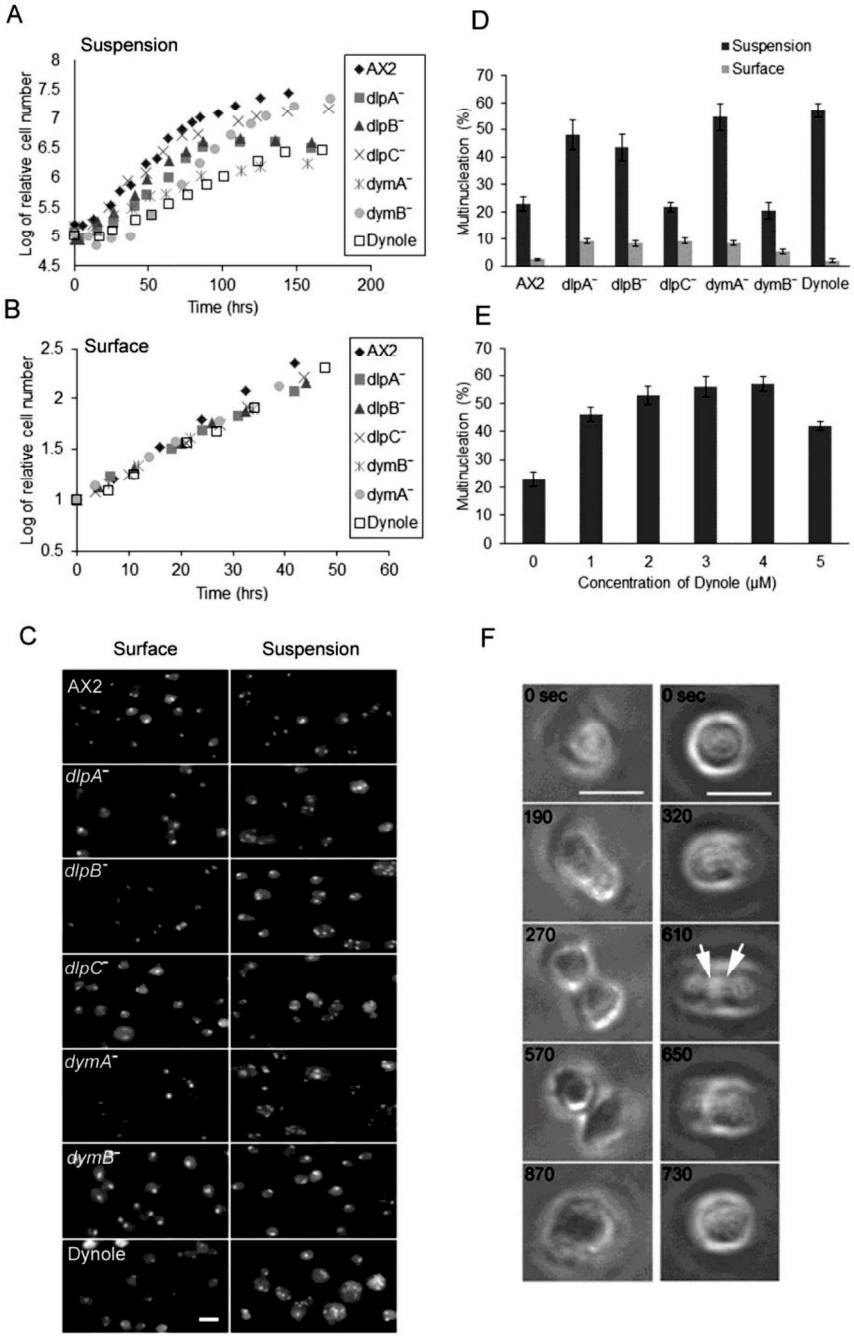
A
Suspension
Log of relative cell number
Time (hrs)
AX2
dlpA⁻
dlpB⁻
dlpC⁻
dymA⁻
dymB⁻
Dynole
B
Surface
Log of relative cell number
Time (hrs)
AX2
dlpA⁻
dlpB⁻
dlpC⁻
dymB⁻
dymA⁻
Dynole
C
Surface
Suspension
AX2
dlpA⁻
dlpB⁻
dlpC⁻
dymA⁻
dymB⁻
Dynole
D
Suspension
Surface
Multinucleation (%)
AX2
dlpA⁻
dlpB⁻
dlpC⁻
dymA⁻
dymB⁻
Dynole
E
Multinucleation (%)
Concentration of Dynole (μM)
F
0 sec
0 sec
190
320
270
610
570
650
870
730

Fig. 2. Dynamins localized to the cleavage furrow in dividing wild-type and myosin II null cells. (A-H) Cells were fixed and immunostained with antibodies against dynamins. DlpA (A and B) and DymA (C-F) primarily localized to the cleavage furrow until separation of the daughter cells, but DymB (G and H) was diffusely distributed in the cytoplasm. (I-P) Myosin II null cells (HS1) were fixed and immunostained. DlpA (I-L) and DymA (M-P) mainly localized to the cleavage furrow, indicating that localization of dynamins is independent of the presence of myosin II. Bars, 10 μm.

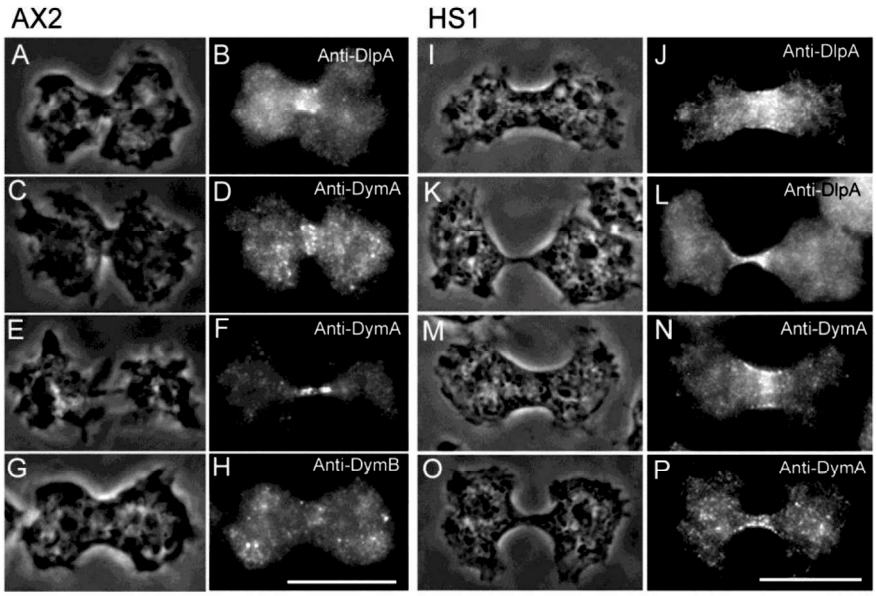
AX2
HS1
A
B
Anti-DlpA
I
J
Anti-DlpA
C
D
Anti-DymA
K
L
Anti-DlpA
E
F
Anti-DymA
M
N
Anti-DymA
G
H
Anti-DymB
O
P
Anti-DymA

Fig. 3. DlpA localized to the cleavage furrow in living cells. (A) A typical sequence of cell division in AX2 cells expressing DlpA-GFP. Note that DlpA-GFP began to accumulate at the equator from late anaphase and remained at the end of cytokinesis. (B) Temporal kinetics of average fluorescence intensity in the brightest area (1 μm in diameter) at the equatorial region of the cell shown in panel A. Fluorescence intensity increased in accordance with the ingression of the furrow. Bar, 10 μm.

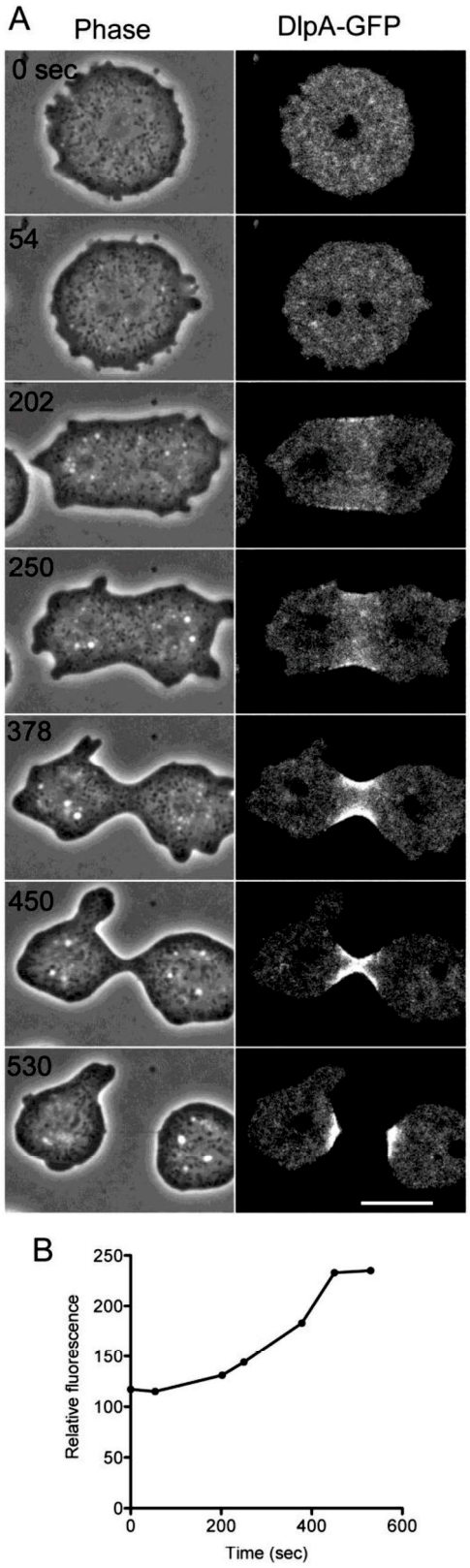
A
Phase
DlpA-GFP
0 sec
54
202
250
378
450
530
B
Relative fluorescence
250
200
150
100
50
0
0
200
400
600
Time (sec)

Fig. 4. Myosin II could not localize properly at the furrow region in dynamin null cells. Dynamin null and AX2 wild-type cells were fixed and immunostained with anti-*Dictyostelium* myosin II antibodies. (A-B) In wild-type cells, myosin II was strongly concentrated at the cleavage furrow. (C-F) Localization of myosin II in *dlpA* null cells. Twenty-six percent (7/27) of the examined cells were indistinguishable from wild-type cells in terms of cell morphology and localization of myosin II at the furrow. However, 41% (11/27) of the mutant cells exhibited almost normal morphology but punctate or patchy myosin localization (C and D). Thirty-three percent (9/27) of the mutant cells presented a swelling or bulge-like structure at the furrow region as well as punctate or patchy myosin localization (E and F). (G-J) Localization of myosin II in *dymA* null cells. Eighteen percent (6/34) of the examined cells were indistinguishable from wild-type cells in terms of morphology and localization of myosin II at the furrow. However, 15% (5/34) of the mutant cells showed normal morphology but punctate or patchy myosin localization (G and H). Sixty-seven percent (23/34) of the mutant cells had a swelling or bulge-like structure at the furrow region and showed punctate or patchy myosin localization (I and J). (K and L) Localization of myosin II in cells treated with 5 μM Dynole. Most of the cells (25/27) exhibited a swelling or bulge-like structure at the furrow region and punctate or patchy myosin localization (K and L). Bar, 10 μm. (M) Relative fluorescence intensity at the furrow region. The average fluorescence intensity at the furrow region was normalized to that of the cytoplasm (mean ± SD). * $p<0.05$, ** $p<0.005$ when compared with AX2.

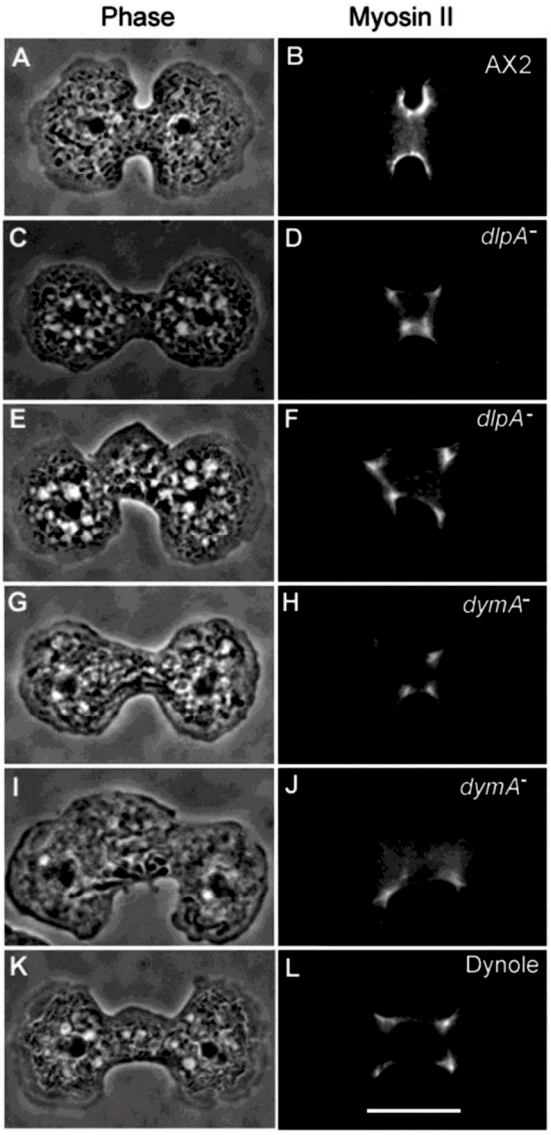
Phase
Myosin II
A
B
AX2
C
D
dlpA-
E
F
dlpA-
G
H
dymA-
I
J
dymA-
K
L
Dynole

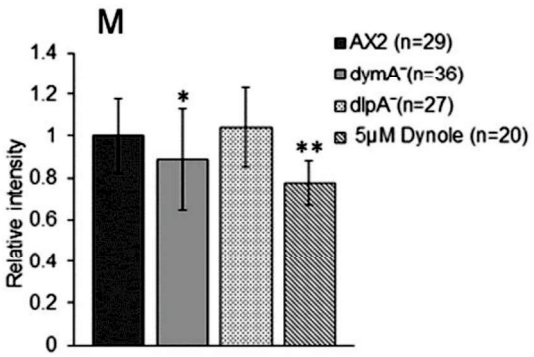
M
AX2 (n=29)
dymA-(n=36)
dlpA-(n=27)
5µM Dynole (n=20)
Relative intensity
1.4
1.2
1
0.8
0.6
0.4
0.2
0
*
**

Fig. 5. Disorganized actin filaments at the furrow of dividing dynamin null cells.

(A) Dividing wild-type and dynamin null cells were fixed and stained with TRITC-phalloidin, and actin filaments were observed under TIRF microscopy. Compared to wild-type cells, disorganized and fragmented actin filaments (arrowheads) were observed in dynamin null cells. White arrows indicate MiDASes. (B) Cells were extracted with an actin-stabilizing buffer containing Triton X-100, and the residual cytoskeletons were stained with antibodies against dynamins and TRITC-phalloidin. DlpA and DymA persisted and colocalized with actin filaments at the cleavage furrow. (C) Western blot detection with anti-DlpA or anti-DymA antibodies: whole cell lysate of wild-type cells (left columns), cell lysate after extraction with Triton X-100 (middle). The loaded number of Triton-treated wild-type cells was 1.5 times of that of whole cell for anti-DlpA blotting and 3 times for anti-DymA blotting, respectively. The right columns shows the absence of DlpA and DymA in whole cell lysate of *dlpA* and *dymA* null cells, respectively. Bars, 10 μm.

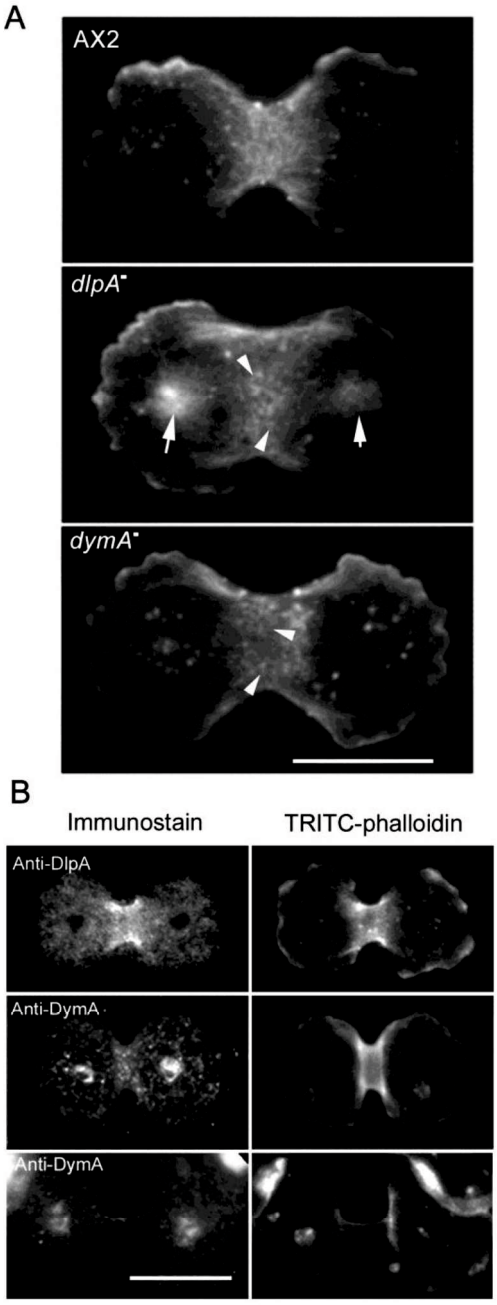
A
AX2
dlpA-
dymA-
B
Immunostain
TRITC-phalloidin
Anti-DlpA
Anti-DymA
Anti-DymA
C
AX2
TX-100
dlpA-
Anti-DlpA
AX2
TX-100
dymA-
Anti-DymA

Fig. 6. DlpA and actin filaments delocalized from the furrow in a similar manner when dividing cells were exposed to latrunculin B. Under confocal microscopy, latrunculin B was applied to dividing cells expressing DlpA-GFP (A) or GFP-ABD 120K (B) at 0 sec. GFP-ABD 120K was used to visualize actin filaments. DlpA-GFP delocalized from the cleavage furrow in a similar manner as GFP-ABD 120 K, and the furrows simultaneously loosened. Bars, 10 μm.

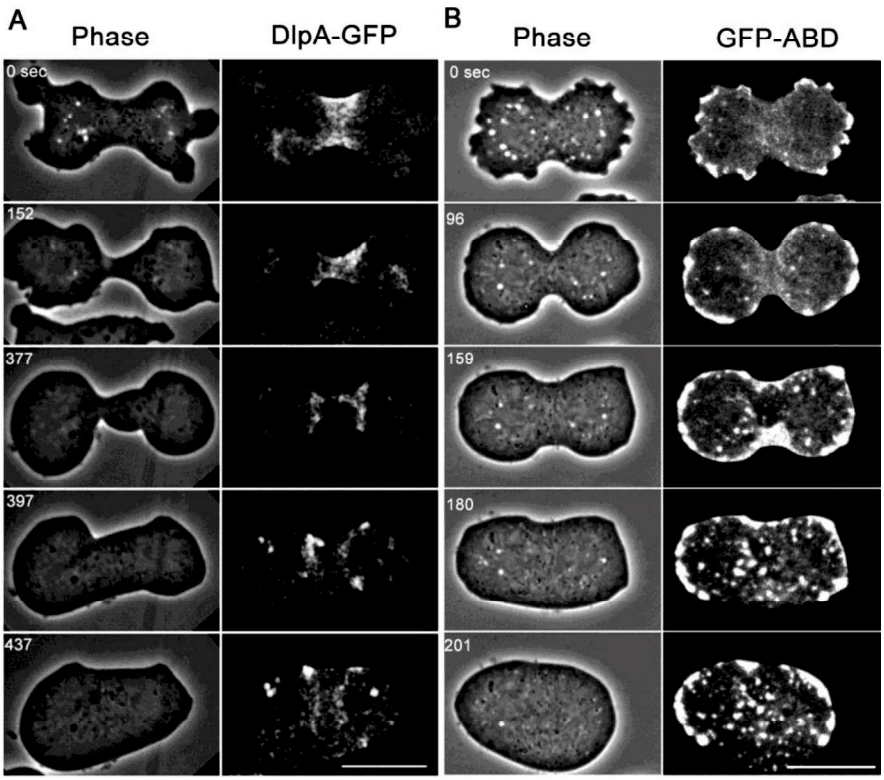
A
Phase
DlpA-GFP
B
Phase
GFP-ABD
0 sec
152
377
397
437
0 sec
96
159
180
201

Fig. 7. Fragmentation of actin filaments at the furrow. (A) Cells were extracted with a buffer containing Triton X-100 and then simultaneously stained with TRITC-DNase I and FITC-phalloidin. Note that the fluorescence intensity of TRITC-DNase I at the furrow of AX2 wild-type cells was significantly lower than that of dynamin null cells, although FITC-phalloidin staining was indistinguishable between the mutant and wild-type cells. (B) Quantitative analysis of the average fluorescence intensity of TRITC-DNase I and FITC-phalloidin at the furrows of wild-type and dynamin null cells. (*$p < 0.001$). (C) Fluorescence at the furrows of *dlpA* null and AX2 wild-type cells expressing GFP-ABD120K was bleached under confocal microscopy. The two panels show fluorescence images taken before and after photobleaching at the furrow. FRAP experiments were performed by focusing specifically on the furrow cortex (optical section of 0.9 μm). The white circle shows the bleached area. (D and E) Representative curves of relative fluorescence recovery of GFP-ABD120K at the furrow in wild-type (D) and *dlpA* null cells (E). (F) Actin filaments turned over significantly more rapidly in *dlpA* null cells than in wild-type cells (*$p < 0.001$). Bars, 10 μm.

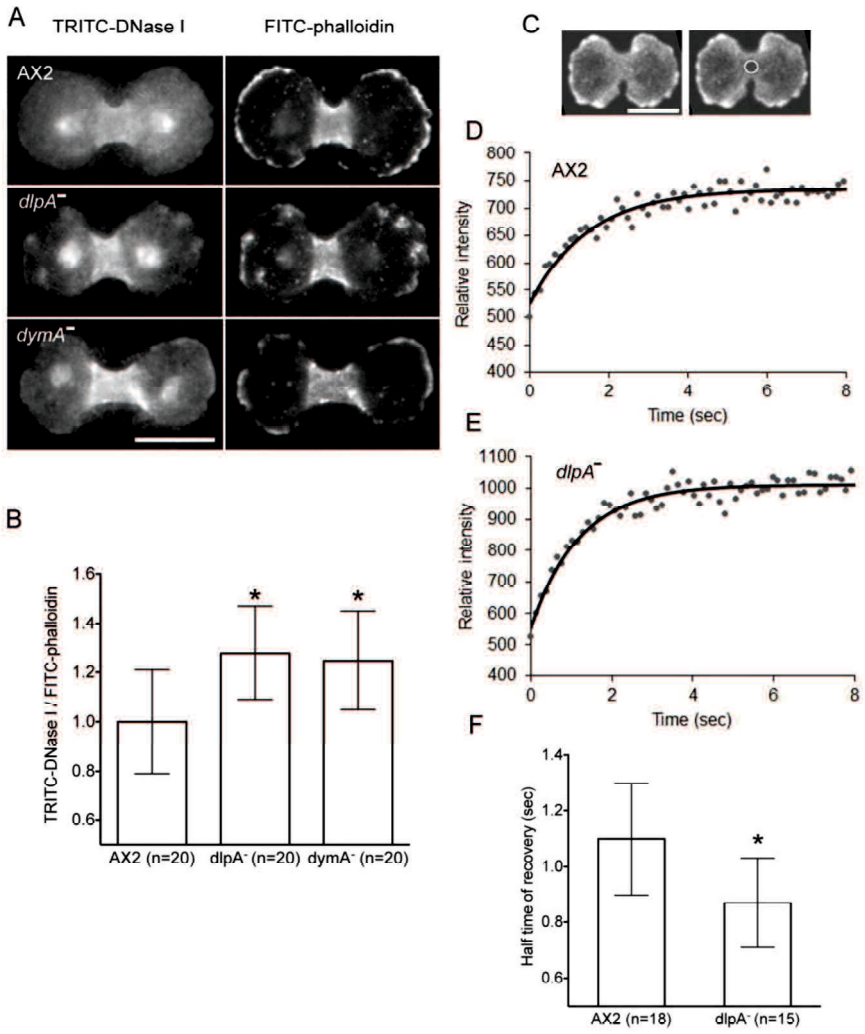
A
TRITC-DNase I
FITC-phalloidin
AX2
dlpA⁻
dymA⁻
B
TRITC-DNase I / FITC-phalloidin
AX2 (n=20)
dlpA⁻ (n=20)
dymA⁻ (n=20)
C
D
AX2
Relative intensity
Time (sec)
E
dlpA⁻
Relative intensity
Time (sec)
F
Half time of recovery (sec)
AX2 (n=18)
dlpA⁻ (n=15)

Fig. 8. Schematic model of actomyosin organization at the furrow. In wild-type cells, dynamin associates with actin filaments to stabilize them at the cleavage furrow (left). Interactions between actin and myosin II filaments cause the contractile ring to constrict and divide the two daughter cells. In dynamin null cells, actin and myosin II are recruited at the contractile ring, but the actin filaments are much shorter in the absence of dynamin. This disparity induces local contraction of the ring, which, in turn, results in patchy localization of myosin II and finally causes the failure of cytokinesis A.

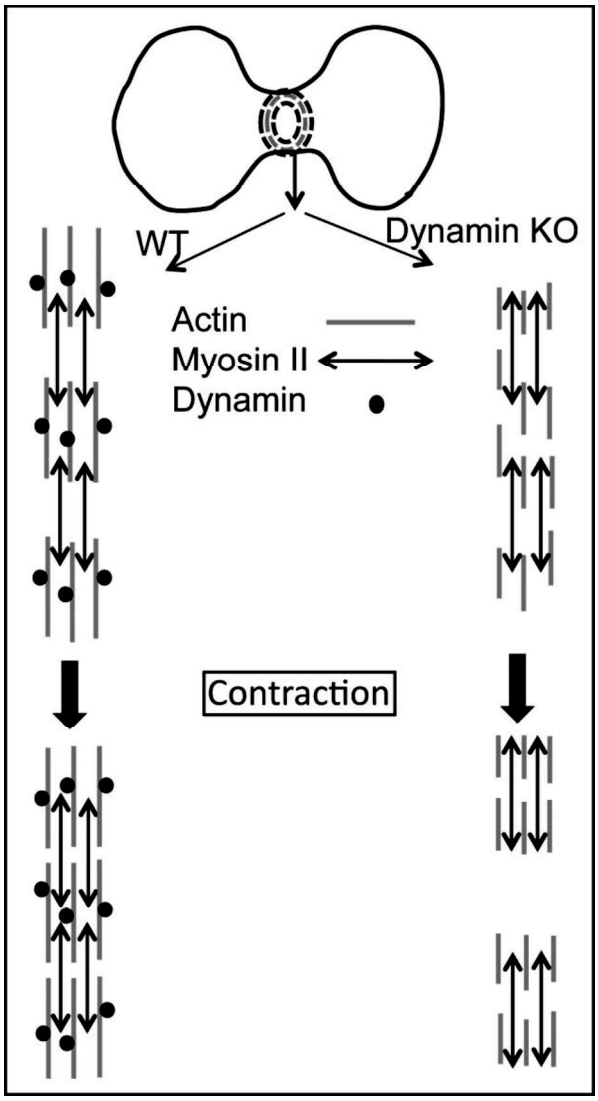
WT
Dynamin KO
Actin
Myosin II
Dynamin
Contraction